Behavior of Surface-Anchored Poly(acrylic acid) Brushes with Grafting Density Gradients on Solid Substrates: 2. Theory

Peng Gong,[†] Tao Wu,[‡,§] Jan Genzer,[‡] and Igal Szleifer*[,†]

Department of Chemistry, Purdue University, West Lafayette, Indiana 47907-1393, and Department of Chemical & Biomolecular Engineering, North Carolina State University, Raleigh, North Carolina 27695-7905

Received May 4, 2007; Revised Manuscript Received August 13, 2007

ABSTRACT: We apply a molecular theory to predict the structural properties of poly(acrylic acid) macromolecules grafted via one of their ends to solid surfaces. The theory explicitly incorporates the acid−base equilibrium responsible for the charge regulation of the acrylic groups, as well as the conformations, size, shape, and charge distributions of all the molecular species present. We compare the predictions of the theory with experimental observations presented in the preceding article for the height of the layer as a function of ionic strength for different polymer molecular weight and polymer surface coverage. The calculated heights are found to be in good agreement with the experimental observations. The theory predicts the distribution of charges within the layer. We find that the counterions adsorb to the grafting surface, overcompensating the charge of the polymer. The charge regulation within the polymer layer is determined by the interplay between the bulk pH, the ionic strength, and the density of polymer. The system tends to become uncharged with decreasing ionic strength of the solution and increasing polymer density. In all cases the charge regulation acts in order to minimize the electrostatic repulsions in the system. The local distribution of protons within the polymer layer is predicted to be very different from that of the bulk solution. The local pH within the polymer layer can be tuned by varying the solution ionic strength and the polymer surface coverage; the variation can be large as two pH units, relative to the bulk pH. This large variation of the local pH within a couple of nanometers within the brush can be used in the design of biosensors.

Introduction

In the previous paper,[1] we presented a systematic experimental study of the behavior of poly(acrylic acid) (PAA) brushes grafted on flat solid substrates and analyzed the results in terms of scaling theories. In the present work, we describe the detailed structure of the polymer layer by comparing the experimental observations with the predictions from a molecular theory. PAA tethered layers represent an example of weak polyelectrolyte brushes made of monomers containing carboxylic acid groups, whose charge depends upon the equilibrium between the charged and uncharged species. In bulk solution, the chemical equilibrium between the charged and uncharged monomers, $AH \leftrightarrow A^- + H^+$, is characterized by an equilibrium constant:[2]

$$K_a = \frac{[A^-][H^+]}{[AH]} = Ce^{-\beta\Delta G^0} \tag{1}$$

where [] denotes the activity, which is usually approximated by the molar concentrations, $\Delta G^0 = \mu^0_{A^-} + \mu^0_{H^+} - \mu^0_{AH}$ is the standard Gibbs free energy of the acid−base equilibrium with μ_i^0 the standard chemical potential of species i, $\beta = 1/kT$ is the inverse absolute temperature, and C is a constant ensuring consistency of units. It is convenient to describe the system in terms of the fraction of charged groups:

$$f = \frac{[A^-]}{[A^-] + [AH]} \tag{2}$$

which is related to the binding constant and the concentration of protons:

$$f = \frac{1}{1 + \frac{[H^+]}{K_a}} \tag{3}$$

The pH at which 50% of the acid groups are dissociated is denoted as pK_a. Concurrently, at pH lower (higher) than the pK_a, the majority of the groups are uncharged (charged). While this always holds true for homogeneous bulk solutions and when the acid groups are present as monomers in solution, the situation is rather different when the acid groups are chemically bound to a polymer backbone. First, the polymeric nature of the molecules changes the fraction of charged monomers with respect to the isolated group.[3] Furthermore, even for an isolated coil in solution, the distribution of charges along the chain depends on the position of the chargeable group along the macromolecule.[4] This is a result of the different electrostatic environment that each monomer feels due to the surrounding monomers from the same chain. Second, as demonstrated by Ninham and Parsegian,[5] charge regulation of acid groups is largely affected by the effect of confinement and inhomogeneous distribution of ions. Therefore, one would expect this effect to be pronounced when the acid groups are incorporated into polymers that are grafted at one of their ends to a surface at a finite surface coverage.

The incorporation of the distance-dependent charge fraction in describing the behavior of polyelectrolyte brushes was first

* Corresponding author. Present address: Department of Biomedical Engineering, Northwestern University, 2145 Sheridan Road, Evanston, IL 60208. E-mail: igalsz@northwestern.edu. Telephone: +1-847-467-0674.
† Department of Chemistry, Purdue University.
‡ Department of Chemical & Biomolecular Engineering, North Carolina State University.
§ Present address: Intel Corporation, Chandler, AZ 85226-3699.

10.1021/ma071018y CCC: $37.00
Published on Web 10/26/2007

introduced by Israëls et al. in their seminal work,[6] in which they generalized the lattice self-consistent field (SCF) theory of Schutjens and Fleer developed originally for neutral polymers.[7] In their work, Israëls and co-workers assumed that the local degree of dissociation can be determined by the requirement that at a given distance from the surface, z, the acid equilibrium constant is the same as in the bulk. Furthermore, Israëls et al. assumed that eq 3 holds but with f and $[H^+]$ replaced by their local values, $f(z)$ and $[H^+(z)]$. This stems from the same ideas put forth by Ninham and Parsegian[5] in their treatment of surface-localized acid groups. The problem with the expression used in the SCF approach[6] is that it is not clear whether the local dissociation obtained in this way is the one that minimizes the free energy. Namely, the bulk equilibrium constant, eq 1, is obtained through the minimization of the system's free energy. Therefore, what is fixed is the free energy of the reaction, ΔG^0. However its relation to the ratio of the local concentrations and thus the local dissociation is not clear.

In this paper, we use a molecular theory recently developed to describe the behavior of weak polyelectrolytes grafted on surfaces of arbitrary geometry.[8] The basic idea is to write down a free energy functional that explicitly includes the ability of the acid groups to dissociate. The degree of dissociation is obtained upon functional minimization of the total free energy. This approach was originally developed to treat uncharged polymer brushes[9] and later generalized for cases in which some of the monomers of the polymers were charged.[10] The predictions of the theory have been shown to be in excellent agreement with full-scale computer simulations[11] and experimental observations[12] for both structural and thermodynamic properties of uncharged polymers. An early application of the theory,[13] using the Israëls et al. approach for the local dissociation,[6] also showed good agreement with experimental observations on PAA. Here we demonstrate that the application of the dissociation gradient model obtained from the full free-energy minimization agrees very well with experimental observations for the PAA brush thickness as a function of solution ionic strength, bulk pH, polymer surface coverage, and brush molecular weight. Furthermore, the molecular theory reveals detailed information about the structural properties of the polymer layer, the variation of the fraction of charge groups as a function of the distance from the surface, and the spatial distribution of counterions, co-ions, and protons. We will discuss later in the paper that the theory predicts that the polymer layer gives rise to an extensive variation in the local pH inside the brush as a function of the distance from surface, onto which the polymers are grafted. These results may have important implications in the design of sensors and in the understanding of chemical reaction in inhomogeneous biological environments.

In the next section we derive the theoretical approach. Section III contains comparisons of the predictions of the theory with experimental observations as well as detailed information on the predicted structure of the polymer layer. Finally, section IV presents concluding remarks.

Theoretical Approach

The basic idea of the molecular theory is to consider each molecular species with all their (nonelectrostatic) intramolecular and surface interactions accounted for in an exact way (for the chosen model system), while the intermolecular interactions are considered within an inhomogeneous mean-field approximation. For example, the polymer chains conformations, i.e., the spatial distribution of the segments in their many possible ways, are explicitly accounted for, and the probability of each conformer

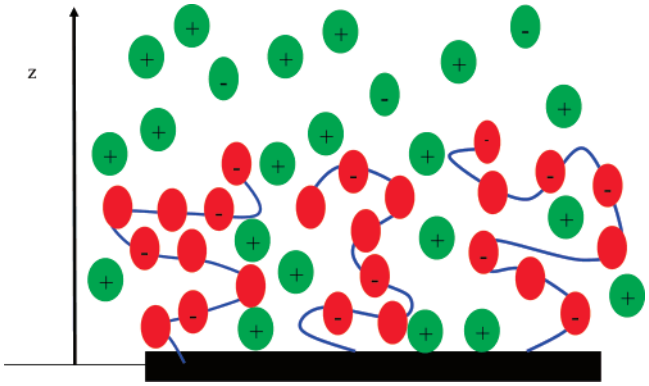

Figure 1. Schematic representation of the weak polyelectrolyte tethered layer. The red monomers with a negative sign represent the A^- groups while those without a sign represent AH. The counter and co ions are drawn in green with their corresponding charge. The blue line connects the polymer segments. The z direction is perpendicular to the surface.

depends on the specific distribution of segments, charge state, and the surrounding environment, due to the intermolecular interactions. This approach enables the consideration of all the relevant interactions, including the coupling between electrostatic, van dew Walls, excluded volume and chemical activity (acid−base equilibrium) well beyond the Poisson−Boltzmann approximation since for all molecular species, the size, shape, conformations and charge distributions are explicitly considered. A detailed description of the implications of the approximations used in this approach with its advantages and limitations can be found in refs 8 and 9.

Consider a system of N_g grafted polymers on a surface of total area A spanning the $x-y$ plane (see Figure 1). The polymers are composed of n segments, each representing an acrylic acid group whose volume is v_p. Each polymer molecule can be found to exist in any of their possible conformations, γ. The polymer is in contact with an aqueous solution containing NaCl salt completely dissociated into Na^+ and Cl^- ions. The bulk concentration of NaCl is c_{salt} and the bulk solution is assumed to have a constant pH.

We assume that the direction perpendicular to the surface is inhomogeneous, and thus the total free energy density, per unit area, can be written as

$$\beta\frac{W}{A}=\frac{N_g}{A}\sum_{\gamma}P(\gamma)\ln P(\gamma)+\frac{1}{2}\int\int\chi(|z-z'|)\langle\phi_g(z)\rangle\langle\phi_g(z')\rangle\,dz\,dz'+\frac{N_g}{A}\int\langle n_g(z)\rangle f(z)[\ln f(z)+\beta\mu_{A^-}{}^0]\,dz+\frac{N_g}{A}\int\langle n_g(z)\rangle(1-f(z))[\ln(1-f(z))+\beta\mu_{AH}{}^0]\,dz+\int\rho_{H^+}(z)[\ln\rho_{H^+}(z)v_w-1+\beta\mu_{H^+}{}^0]\,dz+\int\rho_{OH^-}(z)[\ln\rho_{OH^-}(z)v_{OH^-}-1+\beta\mu_{OH^-}{}^0]\,dz+\int\rho_w(z)[\ln\rho_w(z)v_w-1]\,dz+\int\rho_{Na^+}(z)[\ln\rho_{Na^+}(z)v_w-1]\,dz+\int\rho_{Cl^-}(z)[\ln\rho_{Cl^-}(z)v_w-1]\,dz+\beta\int\left[\langle\rho_q(z)\rangle\Psi(z)-\frac{1}{2}\epsilon\left(\frac{\partial\Psi(z)}{\partial z}\right)^2\right]dz \quad (4)$$

where the first term in eq 4 represents the conformational entropy of the polymer chains, with $P(\gamma)$ denoting the probability distribution function of the chain conformations. The second term accounts for the quality of the solvent. $\chi(|z-z'|)$ is a distance-dependent Flory interaction parameter[14] and $\langle\phi_g(z)\rangle$ is the polymer volume fraction at z. This interaction

parameter corresponds to the mean-field strength of the van der Walls attractions between polymer segments separated by a distance $|z - z'|$. Namely, it is calculated by integrating the contributions for an interaction of the form $1/r^6$, for the polymer segments in the plane z and those in the z' plane.[14] The third and fourth terms in the free energy, eq 4, represent the entropy of mixing and the standard free energy of the charged and uncharged acrylic acid groups, respectively, with $\langle n_g(z)\rangle$ denoting the average number of acrylic acid groups per polymer molecule at z, i.e. between z and $z + dz$, $f(z)$ is the fraction of charged acrylic acid groups at z and the standard chemical potentials are as defined following eq 1. The fifth and sixth terms include the translational and standard free energy of the protons and the hydroxide ions. The seventh to ninth terms represent the translational (mixing) entropy of the water, cations and anions, respectively. $\rho_i(z)$ denotes the density of species i, with $i = w$, Na^+, and Cl^- respectively. The last two terms correspond to the electrostatic contribution to the free energy with $\Psi(z)$ being the electrostatic potential at z.

$$\langle \rho_q(z)\rangle = \frac{N_g}{A}\sum_\gamma P(\gamma) n_g(z;\gamma) f(z) q_g + \rho_{Na^+}(z) q_{Na^+} + \rho_{Cl^-}(z) q_{Cl^-} + \rho_{H^+}(z) q_{H^+} + \rho_{OH^-}(z) q_{OH^-} \quad (5)$$

is the total charge at z and ϵ is the dielectric constant of the medium, which we assume for simplicity to be independent of the composition. The first term in eq 5 corresponds to the polymer contribution with $n_g(z;\gamma)$ being the number of acrylic acid groups that a polymer in conformation γ has at z and $q_g = -1$ is the charge of a dissociated acrylic acid monomer. The second to the last terms in eq 5 correspond to the charge at z of the cations, anions, protons, and hydroxide ions, respectively. We denote the charge of each of the species by q_i even though we describe specific chemical units. The reason for this choice is that the same theory can be applied to other systems with the proper change of chemical identity.

The hard-core repulsive interactions are included through packing constraints, which read:

$$\frac{N_g}{A}\sum_\gamma P(\gamma) v_g(z;\gamma)\, dz + \rho_{Na^+}(z) v_{Na^+}\, dz + \rho_{Cl^-}(z) v_{Cl^-}\, dz + \rho_{H^+}(z) v_{H^+}\, dz + \rho_{OH^-}(z) v_{OH^-}\, dz + \rho_w(z) v_w\, dz = 1 \quad (6)$$

where the first term represents the volume fraction of polymer at z, with $v_g(z;\gamma)\, dz$ being the volume that the polymer chain in conformation γ occupies at z. The next three terms correspond to the volume fraction at z of the anions, cations, protons, hydroxide ions, and water, respectively.

The next step is to determine the density profiles of all the species and the electrostatic potential. This is done by finding the conditions that the free energy, eq 4, subject to the packing constraint, eq 6, and the electroneutrality of the solution, given by $\int[(N_g)/(A)\sum_\gamma P(\gamma) n_g(z;\gamma) f(z) q_g + \rho_{Na^+}(z) q_{Na^+} + \rho_{Cl^-}(z) q_{Cl^-} + \rho_{H^+}(z) q_{H^+} + \rho_{OH^-}(z) q_{OH^-}]\, dz = 0$, is stationary to variations in the probability distribution function, $P(\gamma)$, the density of cations, $\rho_{Na^+}(z)$, anions, $\rho_{Cl^-}(z)$, protons, $\rho_{H^+}(z)$, water, $\rho_w(z)$, the local dissociation of the polymers, $f(z)$, and the electrostatic potential, $\Psi(z)$. Upon introduction of Lagrange multipliers $\beta\pi(z)$, associated with the packing constraints, and the Lagrange multiplier λ, associated with the electroneutrality condition, following some algebraic manipulation, the following relationships for the probability distribution function, different density profiles, and the local degree of dissociation are obtained:

$$P(\gamma) = \frac{1}{q}\exp[-\int \beta\pi(z) v_g(z;\gamma)\, dz - \int\int \chi(|z - z'|) n_g(z;\gamma) \langle \phi_g(z')\rangle\, dz\, dz' - \int [\ln f(z) - \beta\Psi(z)] n_g(z;\gamma)\, dz] \quad (7)$$

$$\rho_{H^+}(z) v_w = \exp[-\beta\mu_{H^+}{}^0 - \beta\pi(z) v_w - \beta\Psi(z) - \lambda] = \rho_{H^+,b} v_w \exp[-\beta(\pi(z) - \pi_b) v_w - \beta\Psi(z)] \quad (8)$$

$$\rho_{OH^-}(z) v_w = \exp[-\beta\mu_{OH^-}{}^0 - \beta\pi(z) v_w + \beta\Psi(z) + \lambda] = \rho_{OH^-,b} v_w \exp[-\beta(\pi(z) - \pi_b) v_w + \beta\Psi(z)] \quad (9)$$

$$\rho_{Na^+}(z) v_w = \exp[\beta\mu_{Na^+} - \beta\pi(z) v_{Na^+} - \beta\Psi(z)] \quad (10)$$

$$\rho_{Cl^-}(z) v_w = \exp[\beta\mu_{Cl^-} - \beta\pi(z) v_{Cl^-} + \beta\Psi(z)] \quad (11)$$

$$\rho_w(z) v_w = \exp[-\beta\pi(z) v_w] \quad (12)$$

$$\frac{f(z)}{1 - f(z)} = \frac{K_a}{\rho_{H^+,b} e^{-\beta\Psi(z)}} \quad (13)$$

$$\frac{\partial^2\Psi(z)}{\partial z^2} = -\frac{1}{\epsilon}\langle \rho_q(z)\rangle \quad (14)$$

where we have explicitly used the negative (positive) charge of the proton (hydroxyl) and cation (anion) and the negative charge of the acrylic group. Further, we have assumed that the volumes of the proton and hydroxyl are the same as that of the water molecule. $\rho_{i,b}$, $i = H^+$ and OH^-, is the bulk density of species i. The specific derivation of these equations is documented in reference.[8]

Several interesting results result directly from the expressions given by eqs 6−14. First, the probability distribution function does not seem to have a clear Boltzmann factor representing the energetic contributions arising from the electrostatic interactions. If that were the case there should be a factor of the form $e^{\beta\int f(z)\Psi(z) n_g(z) dz}$. However, we find that due to the coupling between the electrostatic potential and the fraction of charged groups the final probability includes a seemingly pure electrostatic term associated with all acrylic groups and a reduction of the electrostatic interactions due to the acid−base equilibrium appearing as an entropic-like term. However, there are two contributions that are coupled through eq 13, one containing the bare electrostatic contribution and the other including the chemical equilibrium. Algebraic manipulation of the two contributions leads to the pdf presented in eq 6. Similar results for the combination of electrostatic interactions and chemical equilibrium were presented by Borukhov et al.[21] Second, the local degree of dissociation is *not* given by the relationship found for bulk isotropic solutions, eq 3, replacing the concentration of protons by their local value, as assumed in the SCF approach of Israëls et al. and used by us in early work. This is important because eq 3 assumes that the equilibrium constant K_a is a fundamental constant, and thus the first equality in eq 1 is valid even if the concentrations are the local ones. The minimization of the free energy, including the local dissociation, provides a z-dependent variation of the concentration ratios that depends on the local environment. Note though, that the local environment is determined by the strong nonlocal coupling between the different z's as clearly manifested, for example, in the pdf of chain conformations, eq 6. This implies that the fields $\beta\pi(z)$ and $\Psi(z)$ are not determined only by the properties at z, but each z value is coupled to the whole system. The inhomogeneous environment affects the acidity of the groups due to the varying intermolecular interactions and electrostatic potential. As we will see later, the change in the tendency to dissociate manifests itself in large variations in the local pH inside the grafted layer.

At this point, it is important to emphasize that the local dissociation used by Israëls et al. is the correct one that would be obtained for a lattice model in which the uncharged species has a volume that is identical to the sum of the two charged ions. Our result is more general since it enables any combination of volumes, and therefore we are able to consider chemical detail that is not possible in a lattice model. The particular case that we discuss in this work, as manifested in eq 13, assumes that the proton in solution is in the form of H_3O^+ and thus has the same volume as a water molecule, while A^- and AH have the same volume. Third, eq 14 can be thought of as a generalized Poisson−Boltzmann expression since the charge densities appearing in the right-hand side of eq 14 explicitly include, through eqs 7−13, the size, shape, conformation, charge distributions, and intermolecular interactions between all the molecular species.

This molecular density-functional-self-consistent-field approach incorporates explicitly the coupling between the electrostatic interactions, the conformation statistics of the polymer molecules, the intermolecular van der Waals and excluded volume interactions, and the chemical equilibrium of the acid groups. Furthermore, due to the specific incorporation of the size, shape, and conformations of the molecules we include correlations that go beyond common mean-field approaches.[15] The advantages and limitations of the theory and its application for polymer molecules in inhomogeneous environments have been discussed in detail in refs 8 and 9.

The application of the theory requires the evaluation of the lateral pressure profiles, $\beta\pi(z)$ and the electrostatic potential profile, $\Psi(z)$. From their knowledge, we can determine the distribution of all charged species as a function of the distance from the surface, eqs 8−12, the local degree of dissociation, eq 13, and any average conformational property of the polyelectrolytes, through the use of the probability distribution function, eq 7. To this end, we replace the explicit forms of the density profiles, the probability distribution function and the local dissociation in the constraint equation, eq 6, and the right-hand side of the Poisson equation, eq 14, using eq 5 for the local charge density. The resulting equations are discretized for their numerical solution, as shown and discussed in ref 8. The input necessary to solve the equations includes the following: the polymer surface coverage, the bulk salt concentration, the bulk pH, the acid equilibrium constant in the bulk homogeneous solution, the molecular models for the anion, cation, hydroxyl, proton, and water, and the conformations of the polymer molecules.

The polymer chain conformations were generated using a rotational isomeric state model, in which each segment can have one of three isoenergetic states; see ref 9. The bond length is $l = 0.3$ nm, and the typical number of independent, self-avoiding, conformations that are generated by simple sampling is 5×10^5. The chain conformations are generated once, for each conformation the distribution of volumes and charges is stored and they are used in all the calculations when the sums over conformations are required, see, e.g., eq 6. The ions are modeled as spheres of diameter 0.4 nm. A water molecule has a volume $\upsilon_s = 0.03$ nm^3. The protons and hydroxyl groups have the same volume as water. The p$K_a = 5$ is used for the acrylic groups in the polymer chains. We assume that water is a Θ solvent for the PAA, and the values of the interaction parameters for this solvent condition can be found in ref 14. The other conditions are as stated in the Results.

Results

In the preceding paper, we showed how the structural properties of the grafted PAA layer depend on polymer surface coverage, bulk pH, and ionic strength. Here we start with a direct comparison of the experimental and calculated data, and we follow that with a microscopic description of the structure of the layer, the local degree of dissociation, and description of charge distribution in the system. In this way, we obtain a complete picture of the structure of the polymer layer that goes well beyond properties that can be experimentally accessed.

Figure 2 displays the comparison of the predictions from the theory with the experimental observations for the height of the brush as a function of bulk salt concentration for two different PAA molecular weights and a variety of surface coverage and bulk pH. The height of the polymer layer from the theory is determined as the first moment of the volume fraction distribution. Namely, $\langle h \rangle = \int z\langle\phi_g(z)\rangle\, dz / \int \langle\phi_g(z)\rangle\, dz$. In our experiments, the brush height was deduced by fitting the ellipsometry data to a simple "box" model, which does not accurately account for the shape of the concentration profile (see Figure 3 below). In order to compare the experimental and calculated heights, we determine a scaling factor between the two heights (chosen by applying to the data at 0.25 M) and use the same factor in comparing the heights at all other ionic strengths. As demonstrated by the data in Figure 2, the qualitative comparison between the experiment and the theory is excellent; for instance, the theoretical predictions can faithfully reproduce the occurrence of the maximum in the height in the crossover from the salted brush regime to the osmotic brush regime. From the data in Figure 2, it is apparent that the height of the layer in the high salt regime (quasi-neutral brush) is higher in all cases than that of the neutral brush regime found at very low salt concentrations. We will discuss the origin of this behavior below when we show the detailed structures of the polymer layers.

In spite of the simplicity of the fitting model, the experimentally determined heights are in a very good agreement with the calculated ones for all cases except the highest pH. This demonstrates that the theory is capable of capturing the main variations of the structure of the tethered polymer layer upon changes in surface coverage, pH, molecular weight, and ionic strength. This indicates that the coupling that exists between these interactions is properly treated.

Before discussing the structural features of the polymer layer we need to address the lack of agreement in the experimental observations and theoretical predictions at pH = 10. In this case, the PAA behaves as a strong polyelectrolyte with all the groups charged. Therefore, the maximum observed in the experimental observations cannot be due to the different regimes characteristic of weak polyelectrolytes. The reduction of the layer thickness at low salt concentration is due to counterion condensation. Here the distance between charges for fully charged PAA is smaller than the Bjerrum length (l_B). Therefore, one would expect that once the Debye length (λ_D) becomes comparable to l_B Manning-like condensation will take place. The model cannot predict faithfully the layer collapse at low salt concentrations for the fully charged polymers, because the theoretical approach as presented here does not include counterion condensation. The extension of the theory to include this effect has been recently presented.[16] The predictions of the theory with counterion condensation are in very good agreement with full scale Monte Carlo simulations. The calculations demonstrate that counterion condensation affects film thickness that is qualitatively the same as the experimental observations shown for pH = 10. The comparison between the theory and experiments in the case in

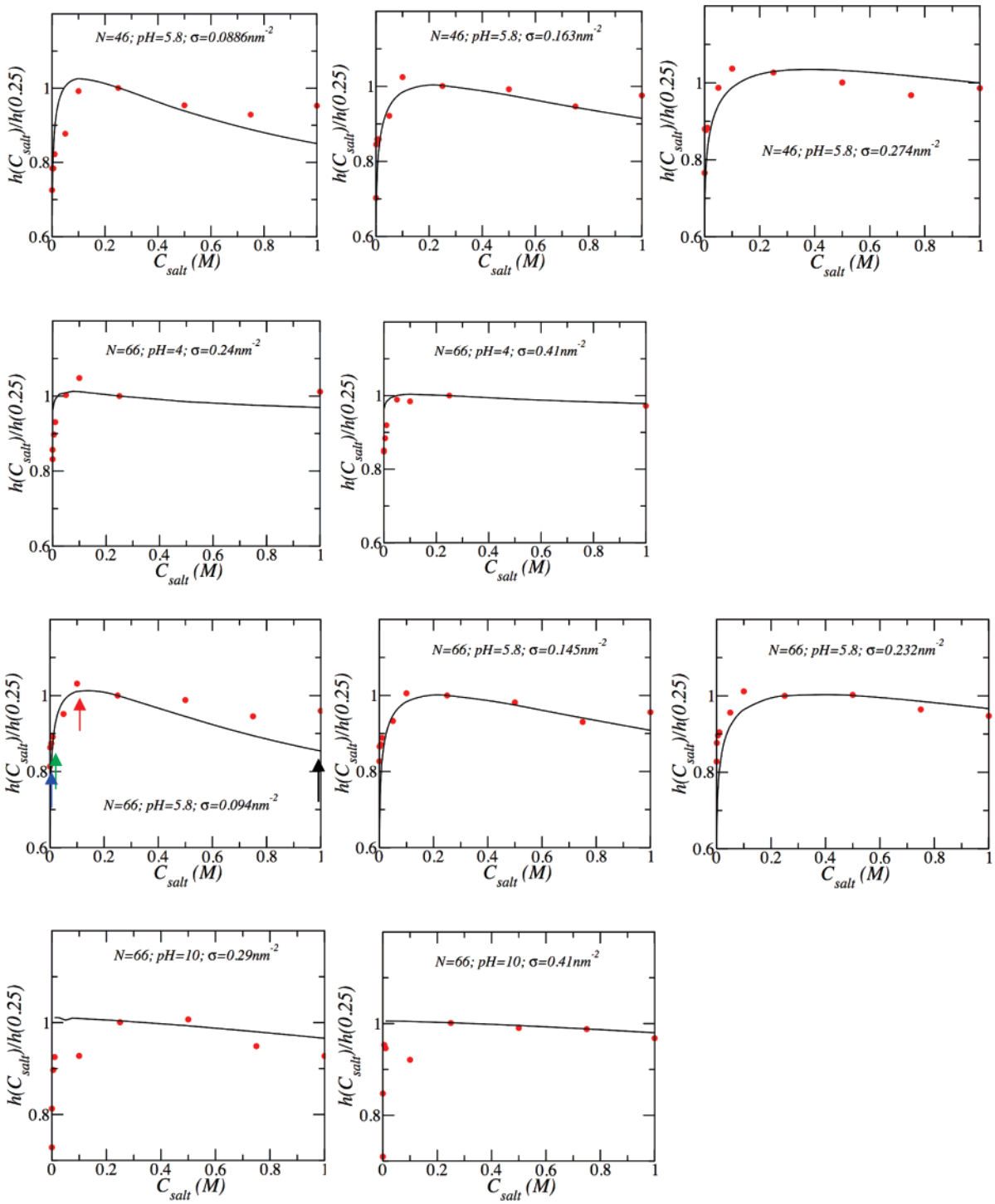

Figure 2. Height of the grafted polymer layers, scaled by the height at $C_{salt} = 0.25$ M, as a function of the bulk salt concentration for the conditions presented within each graph. The symbols are the experimental observations and the lines are predictions from the molecular theory. The arrows mark the salt concentrations described in Figure 3.

which counterion condensation is present is beyond the scope of the work presented here and hence will not be discussed here.

We have chosen one PAA chain length and bulk pH to demonstrate the changes in the structure of the layer and in the local charge, dissociation, and pH for varying solution ionic strength. Figures 3 depicts the polymer density profiles for four different bulk salt concentrations, together with the degree of dissociation of the acrylic groups as a function of the distance from the surface. The chosen values are marked by arrows in the corresponding height profiles in Figure 2; they correspond to a high salt concentration, an intermediate one (in the region of the thickness maximum in Figure 2), and two low salt concentrations. The density profiles reveal that the layer at high salt concentration is stretched. This is due to the large charge density on the polymer as shown in the degree of dissociation. Note that even though the bulk dissociation for the pH and pK_a is $f_{bulk} = 0.86$, most of the polymer has a lower degree of dissociation, which is due to the coupling with the local polymer density and counterion distribution. Namely, due to the finite polymer density, there is an increase in the charge repulsion (very large local charge) and charge regulation takes place in order to reduce the overall free energy of the system. In other words, the chemical equilibrium is shifted to the uncharged species. Because of the large salt concentration, i.e., short Debye

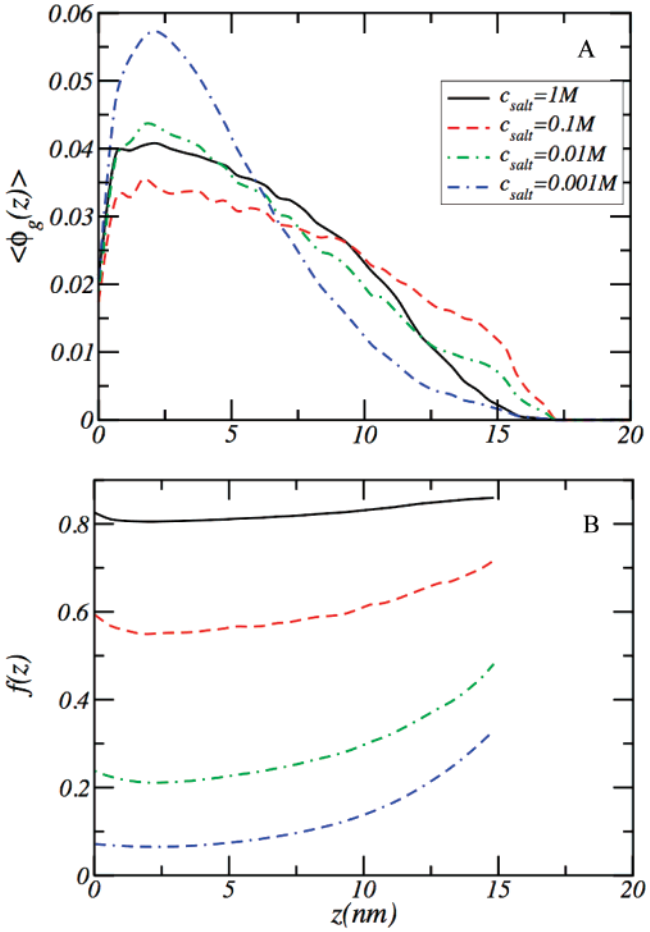

Figure 3. (A) Polymer volume fraction profiles for four different bulk salt concentrations, as denoted in the legend. (B) Degree of dissociation of the acid groups as a function of the distance from the surface for the same four cases shown in the upper graph. In all cases, $N = 66$, pH = 5.8, and $\sigma = 0.094$ nm^{-2}. The four cases are marked by the arrows in Figure 2.

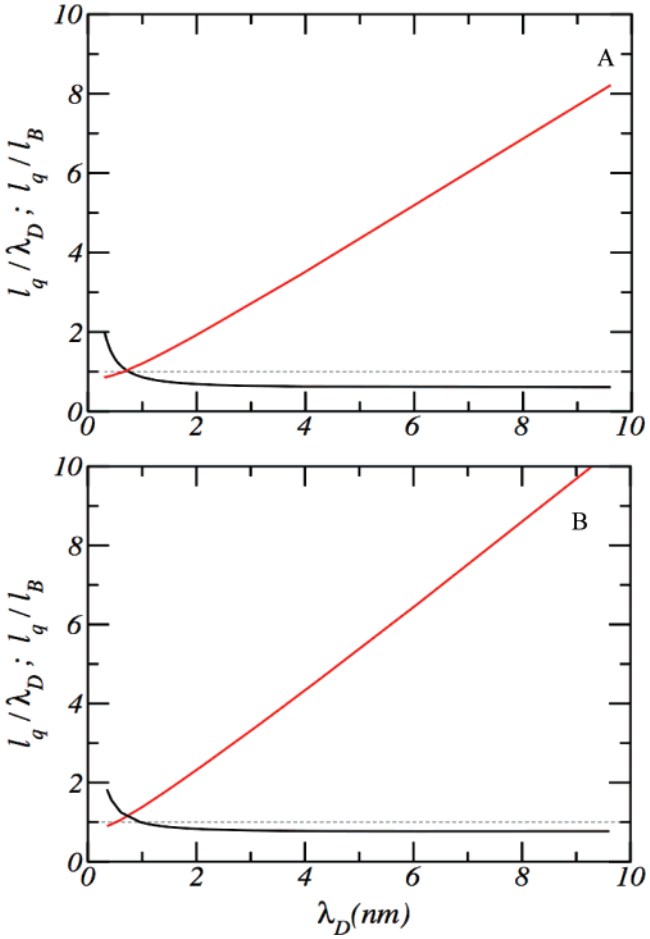

Figure 4. Average distance between charged groups scaled by the Bjerrum length (l_B, red curves) and scaled by the Debye length (λ_D, black curves) as a function of the Debye length. Both cases correspond to $N = 66$, pH = 5.8. Key: (A) $\sigma = 0.095$ nm^{-2}; (B) $\sigma = 0.145$ nm^{-2}.

length and weak electrostatic repulsions, this effect is relatively small and therefore it causes only minute changes in the local dissociation.

For $c_{salt} = 0.1$ M, the polymer layer exhibits the maximum in height in Figure 2; Figure 3 shows a highly stretched polymer layer. This maximal stretching is found even though the polymer layer has a relatively low degree of dissociation. At this point it is important to compare the different relevant length scales that determine the interplay in the electrostatic interactions. The Bjerrum length (l_B) is 0.714 nm, and the distance between acid groups in our model PAA is 0.3 nm; the Debye length (λ_D) is 0.3 nm for 1 M and 0.96 nm for 0.1 M. For a salt concentration of 1 M, the screening is so strong that electrostatic interactions do not play a major role. However, at 0.1 M the $\lambda_D > l_B$, and therefore, electrostatic repulsions between the charged polymer segments become relevant. This is the source of the polymer stretching in reducing the bulk salt concentration from 1 to 0.1 M. The interesting feature is that together with the increase in the role of the electrostatic repulsion, the system has the opportunity to regulate the polymer charge and reduce some of the effect that arises from increasing the strength of the electrostatic interaction through the reduction of salt.

The two lower salt concentrations shown in Figure 3 reveal a further collapse of the polymer layer that results from the decrease in the degree of charge of the polymer layer. At these salt concentrations the more dominant role of the bulk ionic strength is to reduce the charge of the polymer. Namely, the salt plays a dual role of screening the electrostatic interactions and regulating the polymer charge. The very low charge of the polymer implies that the dominant role at these salt concentrations is the charge regulation.

Another way to look at the charge regulation and the competing length scales is to determine the average distance between charges in the polymer and compare it to the Debye and Bjerrum lengths. This comparison is expected to determine the level of charge regulation. As can be seen in Figure 3, the degree of dissociation depends on the distance from the surface. However, in order to be able to have a single average number that enables a simpler comparison, we determine the average distance between charges in the polymer in the following way. We calculate the weighted average fraction of charged groups by multiplying the average charge in the polymer $\langle f \rangle = \int f(z)\phi(z)\,dz/\int \phi(z)\,dz$ by the distance between acrylic groups, i.e. $l_q = \langle f \rangle l$. Figure 4 depicts the average distance between charges as a function of the Debye screening length (λ_D). Specifically, Figure 4 displays two curves: In one of them the average distance between charges is scaled by the Bjerrum length (l_B), while in the other the average distance between charges is scaled by λ_D. We can see that the distance between charges increases with increasing Debye length, reaching a linear regime for $\lambda_D \geq 2$ nm. Thus, l_q/λ_D reaches a plateau for these large values of the Debye length. This is the regime in which the polymer layer becomes more compact, and the thickness decreases with decreasing ionic strength (see Figure 2).

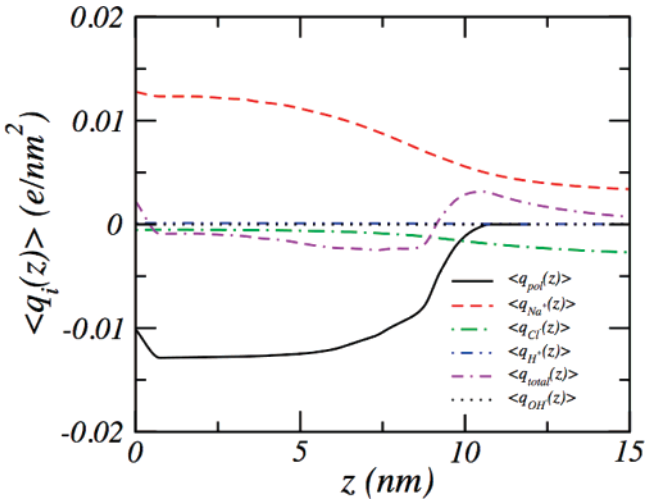

Figure 5. Contribution to the charge as a function of the distance from the surface for each charged moiety. Also shown is the total charge at each distance from the surface. The calculations correspond to $N = 66$, pH = 4, $\sigma = 0.145$ nm^{-2}, and $C_{salt} = 0.01$ M.

One interesting result observed in Figure 4A is that the value, where the distance between charges becomes larger than the Bjerrum length, is very close to the point where $\lambda_D = l_B$ (dashed line in Figure 4). Considering that λ_D is a measure of the range of the electrostatic interactions (screening), in cases where $\lambda_D < l_B$ the Debye length is the only relevant scale. However, when $\lambda_D > l_B$ both length scales are relevant. The results in Figure 4 demonstrate that the charge regulation will always occur in order to maintain the average distance between charges such that the electrostatic repulsions between charged groups is smaller than the thermal energy. As will be argued later this effect can be related to Manning condensation.[16]

The role of surface coverage is clearly seen by comparing the crossover of the curves in Figure 4, parts A and B. For the high surface coverage case, $\sigma = 0.145$ nm^{-2}, the distance between charges is larger for all ionic strengths relative to the low surface coverage cases. This behavior results from charge regulation due to electrostatic repulsions between neighboring chains. This demonstrates the strong coupling that exists between acid−base equilibrium, ionic strength and polymer surface coverage. The curves in Figure 4B cross at λ_D, which is much larger than the l_B. The Debye length of the crossing point increases with increasing polymer surface coverage (results not shown). The curves cross at the Bjerrum length for a single isolated polymer chain, where the only determining factors are the intramolecular electrostatic interactions.

A question that arises is as follows: What is the charge distribution within the polymer layer? Namely, how do the different charged species (polymer segments, anions, cations, hydroxyl groups and protons) get distributed inside the brush as a function of the distance from the surface? In Figure 5 we plot the distribution of those charged moieties, as well as the total local charge, as a function of the distance from the surface. The curves in Figure 5 have been calculated for the following set of parameters: $N = 66$, $\sigma = 0.145$ nm^{-2}, pH = 4, and $c_{salt} = 0.01$ M. We note, however, that qualitatively similar behavior is observed for all other cases considered.[22] One of the most interesting effects observed in all charge distributions that we have calculated is that there is an excess of cations in the close vicinity of the surface. The cation segregation is not driven by charges originating from the surface as in our case the surfaces are uncharged (see our previous paper).[1] We can see from Figure 5 that the total charge starts positive in the surface, indicating

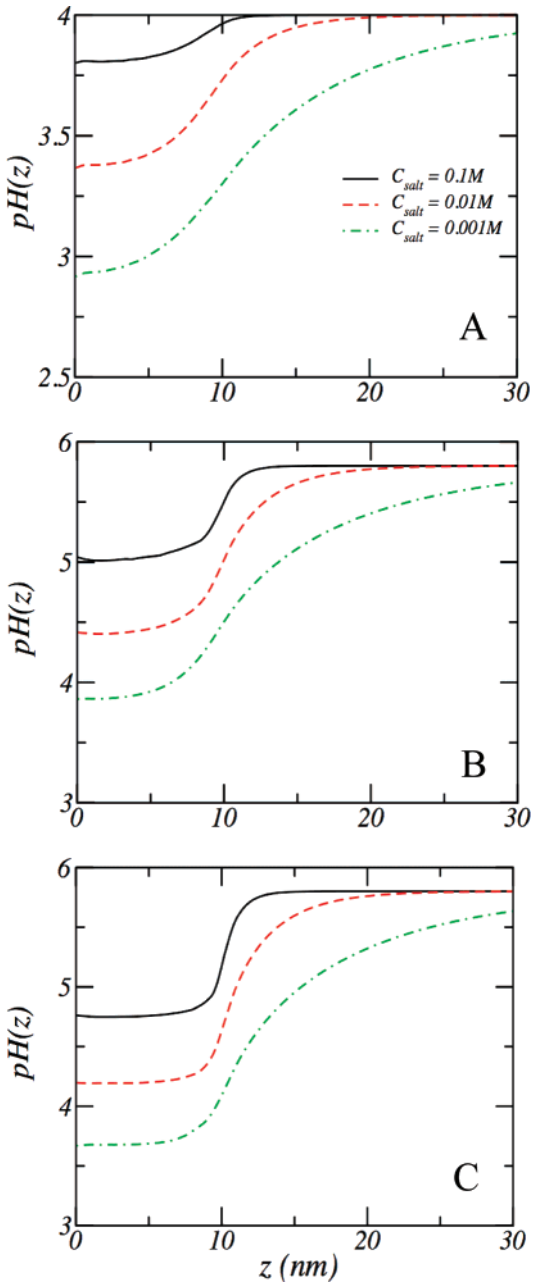

Figure 6. Local pH, pH(z) = −log[H$^+$(z)], as a function of the distance from the surface. Key: (A) bulk pH = 4, $N = 66$, $\sigma = 0.14$ nm^{-2}; (B) bulk pH = 5.8, $N = 66$, $\sigma = 0.09$ nm^{-2}; (C) bulk pH = 5.8, $N = 66$, $\sigma = 0.30$ nm^{-2}.

the adsorption of the polymer counterions in an amount that goes beyond what is needed to neutralize the polymer close to the surface. Furthermore, we also see that at the tip of the brush there is an excess of cations making the two brush "surfaces" charged positively, even though the polymer itself is negatively charged. While the excess charges are in all cases rather small, their behavior is systematic. We find that there is a large adsorption of counterions into the polymer brush, as expected, which help to neutralize the local charge and thus optimize the electrostatic interactions within the brush. At a distance of 10 nm from the surface, corresponding to the distance, to which the polymer layer extends, there is a decay of the charge that is characteristic of an electrostatic double layer and it is due to the slight overall excess positive charge within the polymer layer.

The final result we present is the distribution of protons, or the local pH, as a function of the distance from the surface.

There are nine different cases displayed in Figure 6, corresponding to varying bulk pH, ionic strength, and polymer surface coverage. For a fixed polymer surface coverage and bulk pH, the reduction of the pH within the polymer layer is larger as the ionic strength decreases. This is the result of the protons playing a more important role as counterions of the negatively charged polymers as the concentration of ions arising from the salt decreases. It is important to emphasize that while the relative role of the protons as counterions increases, their overall number within the polymer layer remains low, as can be seen in the distribution of charges presented in Figure 5 and recalling that a pH = 4 corresponds to $[H^+] = 10^{-4}$ M. There are two other trends in the results presented in Figure 6.

The reduction of the local pH with salt concentration increases with increasing solution pH and increasing polymer surface coverage on the surface. The latter effect is weaker than the former one. In all cases, we observe that tuning the solution conditions can lead to large gradients of pH with changes of up to two units, corresponding to 2 orders of magnitude in the proton concentration, within a few nanometers. It is important to note that the changes in the proton local concentration correspond to a constant chemical potential (and activity) of the H^+ at all distances from the surface. The large gradients of proton concentration may constitute an important tool for tuning the reactivity of enzymes, whose activity depends upon the local proton concentration.

Conclusions

In this work, we have presented systematic comparisons of the thickness of the polymer layer between the predictions of a molecular theory to treat weak polyelectrolyte grafted layers and experimental observations on poly(acrylic acid) chains tethered to flat solid surfaces. The predictions of the theory are in good agreement for all experimentally measured polymer surface coverages, chain lengths, pH, and salt concentrations studied with the exception of very high pH. The ability of the theory to predict the variation of the thickness of the polymer layer with salt concentration under so many conditions gives us confidence about the validity of the model for more detailed structural properties. To this end, we studied the detailed structure of the polymer layer under different conditions. Our work predicts, in agreement with earlier work,[6,8,17−20] that the bulk salt concentration plays a dual role in tuning the electrostatic interactions. On the one hand, increasing the ionic strength results in a decrease of the strength and range of the electrostatic interactions. On the other hand, increasing the ionic strength results in a larger charge of the polymer molecules, due to the screening effect of the salt. The quantitative predictions of the local degree of dissociation with salt concentration reveal that weak polyelectrolyte chains can have their charge reduced by more than 80% by changing the salt concentration from 1 M down to 1 mM.

We have established that the change in the local proton concentration can be tuned by changing the solution conditions and the surface coverage of polymers. One can achieve reductions in the local pH by one or two units within a couple of nanometers. The local density of protons results from the interplay between electrostatic interactions, packing and the ability of the polymer segments to regulate their charge. For example, lowering the salt concentration results in an increase of protons within the polymer layer, as they start playing a more important role as counterions. Furthermore, increasing the density of polymers increases the electrostatic repulsions. Attracting protons to the polymer region in order to shift the acid−base equilibrium toward the uncharged species is a mechanism to lower these repulsions. These different scenarios demonstrate that a strong coupling exists between packing, electrostatic interactions and charge regulation. Grafted polymer layers present a unique environment to take advantage of this coupling as one can reach large local densities within a relatively thin film.

The findings relating to the changes in the local pH are very important for the design of nanostructures based on weak polyelectrolytes because they demonstrate that bulk considerations cannot be applied in inhomogeneous regions and even short polymers, such as the ones studied in this work, enable local variations of charges that are orders of magnitude different than their bulk concentrations. These substantial changes in charge distributions and charge regulation can be taken advantage of in designing switches or sensors based on polymer brushes.

We have identified one particular set of experimental conditions, under which the theoretical predictions failed to describe the experimentally observed behavior. Specifically, at very high pH, the polymer chains are completely charged at all ionic strengths. The question that arises then is why there is a reduction of the polymer layer thickness as the salt concentration decreases. The reason stems from counterion condensation due to the large charge on the polymer. Namely, the counterions bind onto the polymer in order to relax the very strong electrostatic repulsions from the very high polymer charge density. The counterion condensation takes place at the very high pH because at those conditions there are not enough protons that would be capable of shifting the chemical equilibrium to the uncharged species of the acrylic acid groups. The theory, as presented in this paper, does not account explicitly for counterion condensation. However, a recent extension of the theory was proposed where counterion condensation was explicitly included in the molecular theory and the predictions where found to be in very good quantitative agreement with full scale Monte Carlo simulations for a lattice polymer.[16] In our future work, we plan to extend the theory for realistic molecular systems which would include the counterion condensation and we will compare the predictions with experimental observations.

Acknowledgment. This work is supported by the National Science Foundation. We thank Dr. Rikkert Nap (Purdue University) for helpful discussions.

References and Notes

(1) Wu, T.; Gong, P.; Szleifer, I.; Vlček, P.; Šubr, V.; Genzer, J. *Macromolecules*, in press.
(2) Atkins, P. *Physical Chemistry*, 6th ed.; W. H. Freeman & Co.: New York, 1998.
(3) Raphael, E.; Joanny, J. F. *Europhys. Lett.* **1990**, *13*, 623.
(4) Castelnovoa, M.; Sens, P.; Joanny, J.-F. *Eur. Phys. J. E* **2000**, *1*, 115−125.
(5) Ninham, B. W.; Parsegian, V. A. *J. Theor. Biol.* **1971**, *31*, 405.
(6) Israëls, R.; Leermakers, F. A. M.; Fleer, G. J.; Zhulina, E. B. *Macromolecules* **1994**, *27*, 3249.
(7) Scheutjens, J. M. H. M.; Fleer, G. J. *J. Phys. Chem.* **1979**, *83*, 1619. Scheutjens, J. M. H. M.; Fleer, G. J. *J. Phys. Chem.* **1980**, *84*, 178.
(8) Nap, R.; Gong, P.; Szleifer, I. *J. Polym. Sci. B* **2006**, *44*, 2638.
(9) Szleifer, I.; Carignano, M. A. *Adv. Chem. Phys.* **1996**, *94*, 165.
(10) Carignano, M. A.; Szleifer, I. *Mol. Phys.* **2002**, *100*, 2993.
(11) Carignano, M. A.; Szleifer, I. *J. Chem. Phys.* **1995**, *102*, 8662.
(12) Faure, M. C.; Bassereau, P.; Carignano, M. A.; Szleifer, I.; Gallot, Y.; Andelman, D. *Eur. Phys. J. B* **1998**, *3*, 365.
(13) Wu, T.; Genzer, J.; Gong, P.; Szleifer, I.; Vlček, P.; Šubr, V. Behavior of surface-anchored poly(acrylic acid) brushes with grafting density gradients on solid substrates. In Polymer Brushes; Brittain, B., Advincula, R., Rühe, J., Caster, K.; Wiley & Sons: New York, 2004.

(14) Carignano, M.; Szleifer, I. *J. Chem. Phys.* **1994**, *100*, 3210.
(15) Solis, F. J.; Olvera de la Cruz, M. *J. Chem. Phys.* **2000**, *112*, 2030.
(16) Hehmeyer, O. J.; Arya, G.; Panagiotopoulos, A. Z.; Szleifer, I. *J. Chem. Phys.* **2007**, *126*, 244902.
(17) Zhulina, E. B.; Birshtein, T. M.; Borisov, O. V. *Macromolecules* **1995**, *28*, 1491.
(18) Zhulina, E. B.; Borisov, O. V. *J. Chem. Phys.* **1997**, *107*, 5952.
(19) Fleer, G. J. *Ber. Bunsen-Ges. Phys. Chem.* **1996**, *100*, 936.
(20) Gong, P.; Genzer, J.; Szleifer, I. *Phys. Rev. Lett.* **2007**, *98*, 018302.
(21) Borukhov, I.; Andelman, D.; Orland, H. *Eur. Phys. J. B* **1998**, *5*, 869.
(22) When the polymers are very slightly charged, one obtains some significant amount of anions within the polymer brush. However, in these cases the density of charges within the polymer layer is very small for all of the components.

MA071018Y